DNA-Hosted Copper Nanoclusters for Fluorescent Identification of Single Nucleotide Polymorphisms

Xiaofang Jia, Jing Li, Lei Han, Jiangtao Ren, Xuan Yang, and Erkang Wang*

State Key Laboratory of Electroanalytical Chemistry, Changchun Institute of Applied Chemistry, Chinese Academy of Sciences, Changchun, Jilin 130022, People's Republic of China, and Graduate School of the Chinese Academy of Sciences, Beijing 100039, People's Republic of China

ABSTRACT

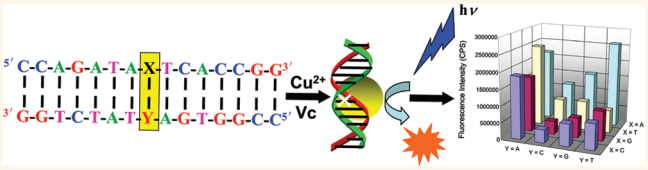

Metal nanoclusters have received considerable interest due to their unique properties and potential applications in numerous fields. Particularly, newly emerging Cu nanoclusters offer excellent potential as functional biological probes. In this work, we for the first time report that the fluorescence of DNA-hosted Cu nanoclusters is very sensitive to base type located in the major groove. This intriguing finding provides a sensitive fluorimetric diagnostic of the mismatch type in a specific DNA sequence, which is difficult to achieve by traditional methods. Furthermore, the research results have shed some light on the luminescent mechanism of Cu nanoclusters. Owing to its high specificity and easy operation without rigorously controlled temperature and arduous probe DNA design, it is expected that the proposed procedure can provide a tool for early diagnosis and risk assessment of malignancy.

KEYWORDS: Cu nanoclusters · DNA recognition · DNA mismatches · fluorescence · DNA duplexes

Noble metal nanoclusters consisting of a few metal atoms, which bridge the gap between traditional organometallic compounds and crystalline metal nanoparticles, are of considerable fundamental interest as well as of potential practical importance.[1] Typically displaying size- and excitation-wavelength-dependent photoluminescence (PL) behavior, noble metal nanoclusters are attracting considerable attention as a fascinating class of fluorophores, particularly for applications in which the size and biocompatibility of the label are critical.[2] Since the first observations of PL from noble metal nanoclusters, great effort has been made to prepare noble metal nanoclusters and explore their potential applications in the subfields of chemical sensing, biological imaging, and *in vitro* bioassays.[2−7] Especially, oligonucleotide-templated nanoclusters have drawn increasing attention due to their facile synthesis, tunable fluorescence emission, high photostability, and suitability as a diagnostic tool for biological concerns.[8−10] Coupling of the excellent PL features with the functionality of the host DNA matrix, these DNA-based fluorescent nanomaterials possess great potential for chemical and biological sensing.[11−14]

Single nucleotide polymorphisms (SNPs) are the most common inherited types of sequence variations in the human genome and are strongly related to various medical and physiological features of human beings. SNP typing that identifies the base at predetermined polymorphic sites in any given DNA sample is envisioned as an essential technology in the near feature for realizing personalized medicine.[15] Therefore, great efforts have been devoted to developing reliable, rapid, and cost-effective technologies for the detection of SNPs.[16−18] DNA biosensors based on simple hybridization recognition provide sequence-specific information by direct or indirect transduction *via* optical, electrochemical, or gravimetric transducers.[19] The prevalent fluorescence-based assays employed for the detection of mismatches in DNA are mainly focused on the complicated covalent modification of the probe oligonucleotides[20−22] and delicate design of ligands that can selectively bind to the mismatched base pairs in duplexes.[23,24] Although still in its infancy, the application of metal nanoclusters in sequence recognition has shown great promise in achieving high selectivity that is difficult to accomplish with conventional methods. Recently, our group elegantly designed cytosine-loop inserted probe DNA strands to hybridize with target DNA strands to form DNA duplex templates for the

* Address correspondence to ekwang@ciac.jl.cn.

Received for review January 17, 2012 and accepted March 14, 2012.

Published online March 14, 2012
10.1021/nn3002455

formation of fluorescent Ag nanoclusters.[25] The formation of fluorescent Ag nanoclusters in these hybridized DNA duplex scaffolds is highly sequence-dependent on the adjacent cytosine-loop sequence and can identify single-nucleotide differences. Newly emerging Cu nanoclusters, which selectively form on DNA duplexes, offer excellent potential as functional biological probes.[26] However, studies focusing on Cu nanoclusters for biological or chemical sensing have been rare to date. In this work, the context of base pairs in the dsDNA host greatly influences the Cu nanocluster environment and hence codes the PL properties. Mismatch-dependent differences in fluorescence are utilized to discriminate different mismatch types at room temperature, highly required in early cancer diagnosis. The correlation of sequence identity with PL property may be useful in other applications such as screening for sequence variation in specific segments of genomic DNA.[27] The research results also provide some useful insight into the luminescent mechanism of Cu nanoclusters. The label-free fluorescent method allows a rapid, simple "mix-and-measure" assay for detection of mismatch type in a DNA duplex without arduous probe DNA design and rigorously controlled temperature.

RESULTS AND DISCUSSION

Synthesis and Characterization of Fluorescent Duplex DNA-Hosted Cu Nanoclusters. In our experiment, briefly, Cu nanoclusters were prepared by reducing $Cu(NO_3)_2$ (100 μM) with ascorbic acid (1.0 mM) in the presence of DNA duplex within 15 min. In contrast to DNA-templated Ag nanoclusters, a higher metal ion/base ratio is nesessary to form Cu nanoclusters effectively. At very low metal ion concentration, Cu^{2+} ions prefer to interact with the backbone phosphate negative groups through nonspecific electrostatic attraction.[28,29] With increasing concentration, the Cu^{2+} ions begin to bind to DNA bases, with much higher affinity than to the phosphate groups, and are further reduced by ascorbic acid to form luminescent Cu nanoclusters. The as-prepared Cu nanoclusters were studied by using UV–vis spectroscopy, PL spectroscopy, transmission electron microscopy (TEM), and atomic force microscopy (AFM).

As shown in Figure 1A, fluorescence studies of Cu nanoclusters revealed that excitation and emission maxima were at 344 and 593 nm, respectively. The characteristic absorption peak similar to the excitation spectrum appeared in the recorded UV–vis absorption spectrum. Moreover, the absorbance band around 560 nm arising from surface plasmon resonance of Cu nanoparticles was not observed, indicating that the sizes of the as-prepared Cu nanoclusters were smaller than 5 nm.[30,31] To further confirm this, a TEM measurement was performed. As expected, the TEM images and the size distribution histograms revealed that the

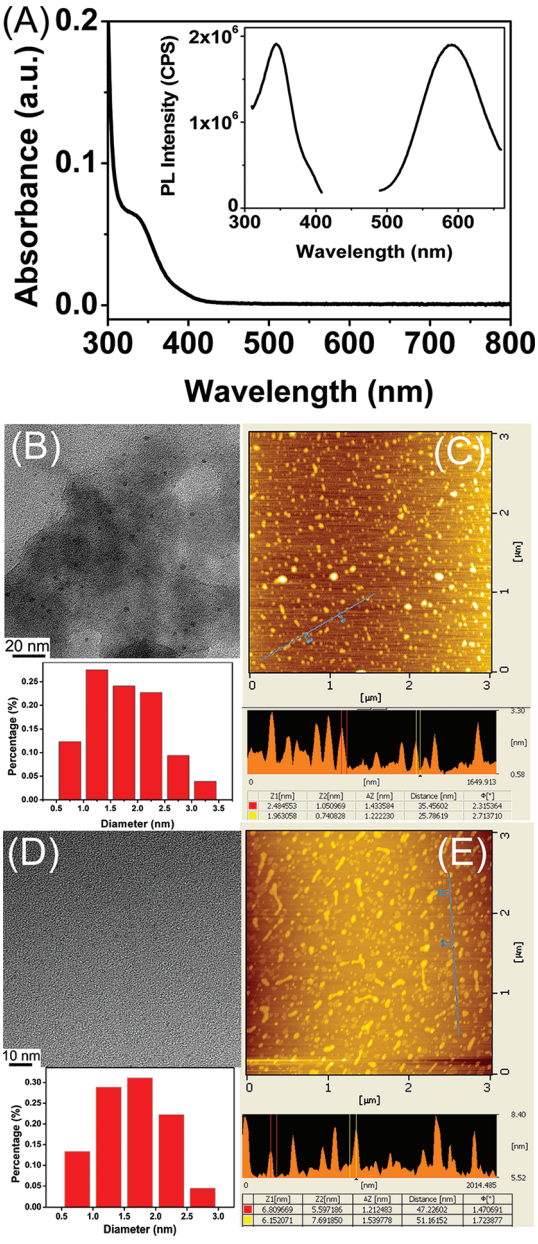

Figure 1. (A) Excitation (measured at λ_{em} = 593 nm), emission (measured at λ_{ex} = 344 nm), and UV–vis absorption spectra of Cu nanoclusters obtained using the FULL duplexes (sequence: 5′-CCA GAT ACT CAC CGG-3′/3′-GGT CTA TGA GTG GCC-5′) as the synthetic scaffold. (B) Representative TEM image and size distribution and (C) representative AFM image of Cu nanoclusters using the FULL duplexes as the synthetic scaffold. (D) Representative TEM image and the size distribution and (E) representative AFM image of Cu nanoclusters using the AC-MIS duplexes (sequence: 5′-CCA GAT ACT CAC CGG-3′/3′-GGT CTA TAA GTG GCC-5′) as the synthetic scaffold.

Cu nanoclusters using FULL and AC-MIS duplexes as the synthetic scaffold were spherical in shape and had average diameters of 1.69 ± 0.62 and 1.69 ± 0.48 nm, respectively (Figure 1B and D). AFM was also recorded to confirm that the average size of the as-prepared Cu nanoclusters was less than 2 nm, consistent with TEM results (Figure 1C and E).

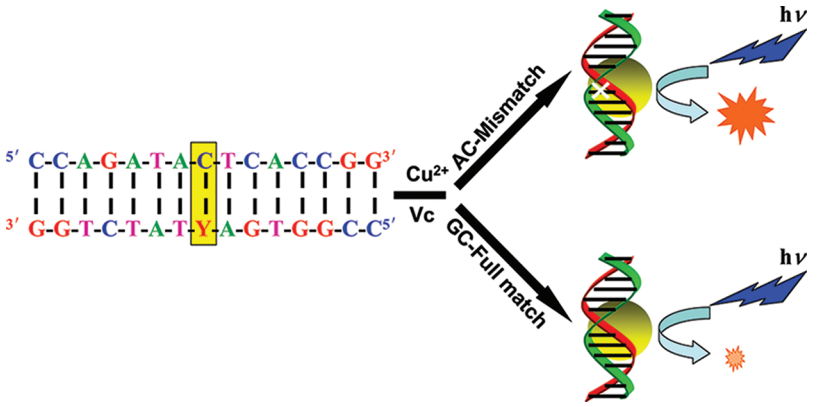

Scheme 1. Schematic representation of detection strategy in our work (Y: SNP site).

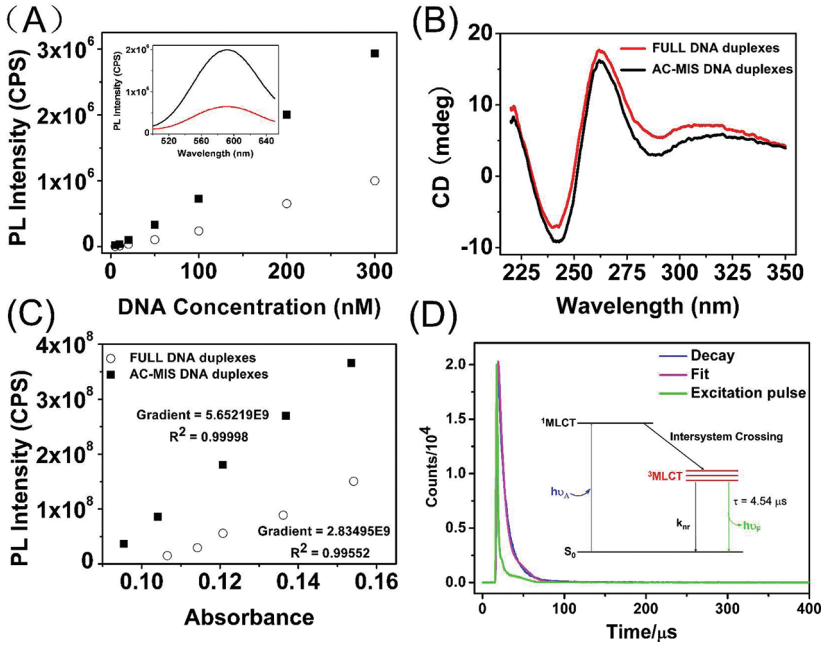

Figure 2. (A) Plots of PL intensity of Cu nanoclusters *versus* increasing concentrations of FULL (○) and AC-MIS (■) duplexes under 344 nm excitation; inset: fluorescence emission spectra of the Cu nanoclusters synthesized with FULL duplexes (red line) and AC-MIS duplexes (black line) under 344 nm excitation; (B) CD spectra for characterizing the structures of FULL duplexes (red line) and AC-MIS duplexes (black line) [2 μM DNA in 20 mM MOPS buffer (pH 7.5) containing 300 mM NaCl]; (C) linear plots for Cu nanoclusters formed by FULL duplexes (○) and AC-MIS duplexes (■); the gradient for each sample is proportional to that sample's fluorescence quantum yield; (D) fluorescence decay profile (λ_{ex} = 340 nm, λ_{em} = 595 nm) of Cu nanoclusters and a possible Jablonski diagram for Cu nanoclusters. The decay time is near 4.54 μs.

Identifying Single-Nucleotide Polymorphisms and Possible Mechanism. Using the intelligent probe Cu nanoclusters, we attempted to detect a hot-spot mutation of G to A, which is found to be present in the genome of patients affected by hereditary tyrosinemia type I.[32] As presented in Scheme 1, the fluorescence of Cu nanoclusters was dramatically enhanced with mismatched DNA: the relative intensity with mismatched *versus* matched DNA was 3-fold (Figure 2A). In addition, the PL intensity was proportional to the concentration of DNA, and the intensity ratio was 3-fold over the concentration range examined. However, as shown in Figure 1, there were no considerable differences between the sizes of Cu nanoclusters obtained using FULL and AC-MIS duplexes as the synthetic scaffold, ruling out the possibility of the formation of the larger Cu nanoclusters. To gain insight into the enhanced mechanism, we obtained circular dichroism (CD) spectra and performed a fluorescence quantum yield study. The CD spectra of FULL and AC-MIS duplexes indicated that structure characteristics of the B-form helix were mainly maintained at room temperature and featured a positive long-wavelength band at 262 nm and a negative band around 242 nm with similar amplitude (Figure 2B).[33] A single-nucleotide mismatch had almost no effect on the conformation of the duplex under the present experimental conditions. However, as depicted in Figure 2C, the fluorescence quantum yield of Cu nanoclusters formed by AC-MIS duplexes was twice that of FULL duplexes, although the absorbance

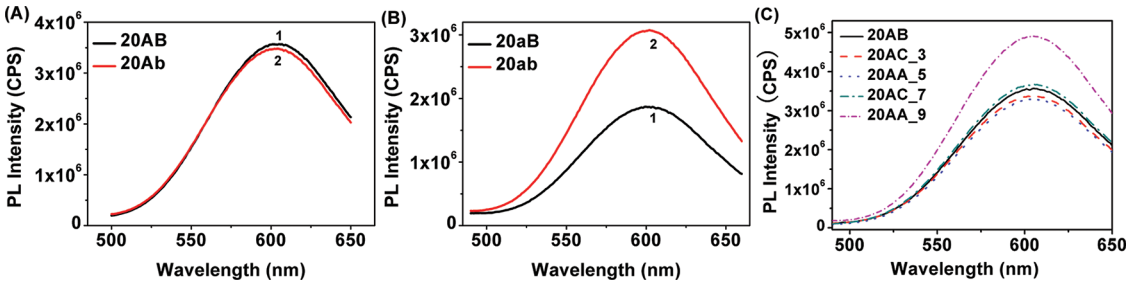

Figure 3. Fluorescence emission spectra of (A) 20AB (1), 20Ab (2), (B) 20aB (1), 20ab (2), and (C) 20AY_n. Conditions: 500 μL of 200 nM DNA in 10 mM MOPS buffer (pH 7.5) containing 150 mM NaCl. DNA sequence: 20AB, 20Ab, and 20AY_n denote probe DNA 20A hybridized with the DNA 20B, 20b, and different mutation site DNA 20Y_n, respectively; 20aB and 20ab denote the truncated 15-base probe DNA 20a hybridized with the DNA 20B and 20b, respectively.

of Cu nanoclusters formed by AC-MIS duplexes was the same or even slightly lower than that of FULL duplexes (Figure S2). These observations suggested that the enhanced fluorescence intensity was because the AC-MIS duplexes could provide an appropriate environment for fluorescent Cu nanoclusters, but not for forming more Cu nanoclusters. The fluorescence lifetime of the formed Cu nanoclusters was measured using a time-correlated single photon counting technique (Figure 2D). The long radiative lifetime in the microsecond range and the large Stokes shift of 249 nm implied that 595 nm emission obtained at 340 nm excitation was derived from triplet excited states, which was similar to general characteristics of luminescent high-nuclearity gold(I) complexes that displayed ligand−metal charge transfer and metal-(I)−metal(I) interactions.[34,35] Jin *et al.* reported that the quantum yield of 25-atom gold nanoclusters [$Au_{25}(SR)_{18}$] was significantly affected by the surface ligands, and they proposed a mechanism of ligand to metal nanoparticle core charge transfer.[36] Such a charge transfer was believed to affect the excited-state relaxation dynamics (*e.g.*, radiative *vs* nonradiative rates). Since surface ligands played a major role in improving the fluorescence of Cu nanoclusters, we inferred that the enhanced fluorescence might originate from the different electron-donating capability of the ligand DNA, similar to gold nanoclusters. Further detailed investigations on the underlying fluorescence enhancement mechanism are still under way.

Mismatch-Dependent Differences in Fluorescence of Cu Nanoclusters and Some Discussion of the Results. In view of the above results obtained with the 15-mer probe DNA, two issues important for further application need to be addressed. First, is the system universal, and do the observed effects depend solely on the length of the designed probe sequence? Second, what is the possible reason for such unusual PL behavior of the system? To address the first issue, a new duplex containing a 20-bp probe strand and target strand was designed. As shown in Figure 3A, there was almost no distinction between full matched DNA 20AB (sequence: 5′-GAA CGA AAC **C**AT TAT ACG AT-3′/3′-CTT GCT TTG **G**TA ATA TGC TA-5′) and one-base-mismatched DNA 20Ab (sequence: 5′-GAA CGA AAC **C**AT TAT ACG AT-3′/3′-CTT GCT TTG *T*TA ATA TGC TA-5′, spot mutation of G-T). In contrast, for the truncated 15-base probe DNA 20a (sequence: 5′-ACG AAA C**A**A TTA TAC-3′), there was an obvious difference (Figure 3B). A shorter probe DNA, such as 10-base DNA, was not suitable, because the 10-mer mismatched DNA exists in a single-stranded form, which cannot serve as an efficient template.[26] Furthermore, as listed in Table S1, parallel studies were carried out using 20-mer DNA 20AY_n (probe DNA 20A hybridized with the different mutation site DNA 20Y_n) as the templates. Figure 3C shows the PL spectra of full matched DNA 20AB and the four one-base-mismatched DNA 20AY_n with different mutation sites. Only DNA 20AA_9, where the dG nucleotide in 20B is replaced by a dA nucleotide in 20A_9, exhibited clearly enhanced fluorescence compared with 20AB. As for the other mutation sites, neglectable PL intensity changes were observed. In the case of probe DNA 15-C (X = C) and target DNA sequence containing a G-A mutation at the end as the template (sequence: 5′-**C**CA GAT ACT CAC CGG-3′/3′-*A*GT CTA TGA GTG GCC-5′), no enhanced fluorescence intensity was also observed. We surmised that the mismatched bases that did not lie in the major groove where the Cu nanoclusters were accumulated[26] had no influence on the fluorescence of the Cu nanoclusters. Altogether, the above results indicated that both the length and the situated mutation position of the designed probe DNA play an important role in the discrimination between the intact and mutated sequence. The truncated 15-mer long variant of designed probe DNA 20a and the right middle mutation spot of DNA 20A_9 allowed favorable discrimination between the fully matched and SNP-containing DNAs.

To address the issue of the possible reason for the unusual PL behavior of the system, the fluorescence properties of Cu nanoclusters formed with all 16 possible base-pair combinations of XY duplexes (XY represents 15-X/15-Y duplexes) were investigated. As depicted in Figure 4 and Figure S3, mismatch-dependent differences in fluorescence were found and

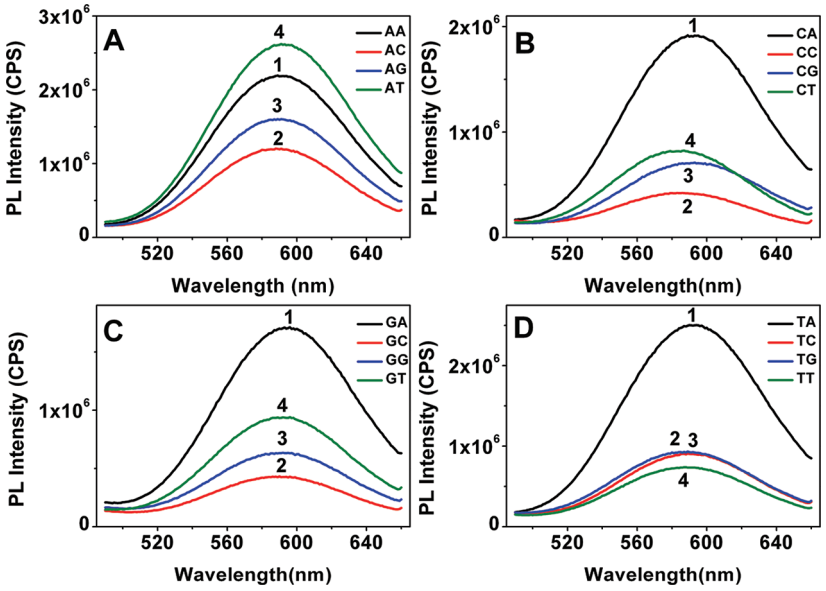

Figure 4. Fluorescence emission spectra of probe DNA 15-X (sequence: 5′-CCA GAT AXT CAC CGG-3′), where X = (A) A, (B) C, (C) G, (D) T, hybridized with the four targets 15-Y (sequence: 3′- GGT CTA TYA GTG GCC-5′) [where Y = A (1), C (2), G (3), or T (4)]. Conditions: 500 μL of 200 nM DNA in 10 mM MOPS buffer (pH 7.5) containing 150 mM NaCl.

the fluorescence intensity deceased in the sequence AT > TA> AA> CA > GA > AG > AC > GT > TG > TC > CT > TT > CG > GG > GC > CC. On the basis of these results, we come to the preliminary conclusion that adenine bases located in the major groove were the most favorable for the fluorescence of Cu nanoclusters, but cytosine and guanine bases were not so conducive to PL. This corresponded with the result as described above that the fluorescence of Cu nanoclusters was dramatically enhanced with AC-MIS duplexes compared with FULL duplexes. The mismatch-dependent differences in fluorescence might originate from different electron donation capability of the ligand base pairs located in the major groove of the DNA scaffold. DNA, as ligands with electron-rich atoms (*e.g.*, N, O) and high affinity for metal cations, can largely promote fluorescence. The sequence of oxidation potentials of the nucleotides is found as dG < dA < dT < dC; therefore, the order of charge-donating capability follows the order dG > dA > dT > dC. Although dG has the lowest oxidation potential among the four nucleotides, it is often detrimental for the luminescence of organic dyes.[37] Instead, dA is generally the least effective as a quencher. Taken together, we infer that the donating capability and the correlation with quenching efficiencies likely act in a coupled and cooperative manner to modify the fluorescent behavior of DNA-templated Cu nanoclusters.

Additionally, the duplexes with different mismatched bases can be best discriminated from others by flexibly choosing probe DNA. For example, different mismatches were clearly distinguishable with the probe DNA 15-X = G. The GA, GT, and GG mismatched duplex-stabilized Cu nanoclusters were 4.2-fold, 2.3-fold, and 1.5-fold of that of full matched GC, respectively (Figure 4C). Overall, our

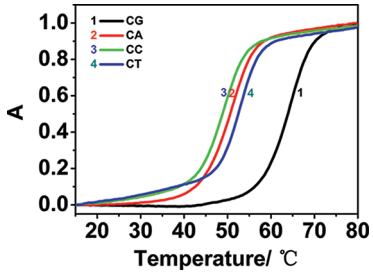

Figure 5. Relative absorbance $A = [(A_t - A_{20°C})/(A_{80°C} - A_{20°C})]$ at 260 nm *vs* temperature for characterizing the structures of full matched CG (1) duplexes and mismatched CA (2), CC (3), and CT (4) duplexes. Conditions: 2 μM DNA in 20 mM MOPS buffer (pH 7.5) containing 300 mM NaCl.

results allowed easy fluorimetric discrimination between them, which was attractive for recognition of different types of mismatches without enzymes.[38]

As shown in Figure 5, thermally induced transition profiles of four duplexes (X = C) revealed that the full duplex formed a more double-helical region than the mismatched duplexes, but the T_m value of the three duplexes containing single-nucleotide mismatch was only slightly distinct. In contrast to previous approaches largely relying on the differences in hybridization efficiency,[39−41] the PL intensity of Cu nanoclusters was not correlated with the thermodynamics of duplex formation, but significantly affected by the type of base pairs. This allowed the rapid, simple "mix-and-measure" detection of mismatch type in a specific DNA sequence at room temperature without rigorously controlled temperature. The result is completely opposite of the previous report that dsDNA containing a single base mismatch did not act as an efficient template for forming fluorescent Cu nanoclusters.[26] Their proposal is

dependent on the fact that the formation of Cu nanoclusters is highly selective for dsDNA compared with ssDNA; namely, the mismatched DNA exists in a single-stranded form, which cannot serve as an efficient template. Unfortunately, it is unpractical for the SNP detection and different mismatch types cannot be discerned, which is required for realizing personalized medicine. As for the two-base mismatch target DNA, the PL intensity was very weak, suggesting the high selectivity of the probe Cu nanoclusters (Figure S4).

CONCLUSION

In summary, using the intelligent probe Cu nanoclusters, we successfully distinguish match and mismatch sequences with 15-mer probe DNA in solution. Since Cu nanoclusters are sensitive to base type located in the major groove, they are excellent fluorimetric indicators of the DNA hybridization event that allows the detection of not only a single mismatch but also its mismatch type in a specific DNA sequence. The research results also provide some useful insight into the luminescent mechanism of DNA-hosted Cu nanoclusters, which is strongly ligand-dependent. In addition, our proposed assay has some unique features: (1) The rapid, reliable "mix-and-measure" detection of mismatch type can be performed at room temperature without rigorously controlled temperature and directly in a duplex without arduous probe DNA design; (2) by flexibly choosing probe DNA, easy fluorimetric recognition of different mismatched types is achieved without enzyme. Armed with these intriguing properties, the emissive metal nanoclusters are expected to open new opportunities for numerous research fields, such as DNA diagnostics, biological recognition, and bioanalysis fields.

EXPERIMENTAL SECTION

Chemicals and Materials. The ultra PAGE-purified and MS-verified oligonucleotides and ultrapure 3-(*N*-morpholino)propanesulfonic acid (MOPS) were obtained from Shanghai Sangon Biotechnology Co. Ltd. (Shanghai, China). Ascorbic acid was purchased from Fluka Chemie GmbH (Switzerland). $Cu(NO_3)_2 \cdot 3H_2O$, NaCl, and other chemicals were purchased from Beijing Chemical Works (Beijing, China). The stock solutions of DNA samples were prepared in MOPS buffer (20 mM MOPS, 300 mM NaCl, pH 7.5), and then DNA concentrations were accurately quantified using the 260 nm UV absorbance and the corresponding extinction coefficient. All the solutions were prepared with water purified by a Milli-Q system (Millipore, Bedford, MA, USA) and stored at 4 °C.

Apparatus. UV−visible absorption spectra were recorded using a Cary 50 Scan UV−visible spectrophotometer (Varian, USA). Fluorescence spectra were collected on a Fluoromax-4 spectrofluorometer (Horiba Jobin Yvon Inc., France). Circular dichroism spectra were collected using a JASCO J-820 spectropolarimeter (Tokyo, Japan). Transmission electron microscopy measurements were made on a JEM-2100F high-resolution transmission electron microscope (The Netherlands) operated at 200 kV. The AFM image was taken by using a SPI3800N microscope (Seiko Instruments, Inc.) operating in the tapping mode with standard silicon nitride tips. The luminescence decay curves were measured on a FLS920 spectrofluorometer (Edinburgh Instruments,UK) equipped with μF 920H μs pulsed flashlamp.

Preparation of Cu Nanoclusters. In a typical hybridization experiment, the stock solutions of probe DNA and target DNA were diluted to desired concentration with the MOPS buffer (20 mM MOPS, 300 mM NaCl, pH 7.5), and then they were mixed at 1:1 molar ratio. The mixture was heated at 90 °C for 10 min, followed by slowly cooling to room temperature (20 °C) in 3 h. Then, 5 μL of 100 mM ascorbic acid was added into 250 μL of DNA duplex solutions. After the solution mixtures were shaken for 30 s, 250 μL of 200 μM $Cu(NO_3)_2$ solution was added and incubated for 15 min at room temperature to form Cu nanoclusters (see Figure S1; Cu nanoclusters were formed in 15 min).

Conflict of Interest: The authors declare no competing financial interest.

Acknowledgment. This work is supported by the National Natural Science Foundation of China with Grants 21190040 and 21075120 and 973 Projects 2010CB933600 and 2011CB911000.

Supporting Information Available: Figures S1−4, Table S1. This material is available free of charge *via* the Internet at http://pubs.acs.org.

REFERENCES AND NOTES

1. Jin, R.; Zhu, Y.; Qian, H. Quantum-Sized Gold Nanoclusters: Bridging the Gap between Organometallics and Nanocrystals. *Chem.—Eur. J.* **2011**, *17*, 6584–6593.
2. Xu, H. X.; Suslick, K. S. Water-Soluble Fluorescent Silver Nanoclusters. *Adv. Mater.* **2010**, *22*, 1078–1082.
3. Tanaka, S.-I.; Miyazaki, J.; Tiwari, D. K.; Jin, T.; Inouye, Y. Fluorescent Platinum Nanoclusters: Synthesis, Purification, Characterization, and Application to Bioimaging. *Angew. Chem., Int. Ed.* **2011**, *50*, 431–435.
4. Zhou, C.; Long, M.; Qin, Y.; Sun, X.; Zheng, J. Luminescent Gold Nanoparticles with Efficient Renal Clearance. *Angew. Chem., Int. Ed.* **2011**, *50*, 3168–3172.
5. Wu, Z. K.; Lanni, E.; Chen, W. Q.; Bier, M. E.; Ly, D.; Jin, R. C. High Yield, Large Scale Synthesis of Thiolate-Protected Ag-7 Clusters. *J. Am. Chem. Soc.* **2009**, *131*, 16672–16674.
6. Rao, T. U. B.; Pradeep, T. Luminescent Ag-7 and Ag-8 Clusters by Interfacial Synthesis. *Angew. Chem., Int. Ed.* **2010**, *49*, 3925–3929.
7. Yu, M.; Zhou, C.; Liu, J.; Hankins, J. D.; Zheng, J. Luminescent Gold Nanoparticles with pH-Dependent Membrane Adsorption. *J. Am. Chem. Soc.* **2011**, *133*, 11014–11017.
8. Richards, C. I.; Choi, S.; Hsiang, J.-C.; Antoku, Y.; Vosch, T.; Bongiorno, A.; Tzeng, Y.-L.; Dickson, R. M. Oligonucleotide-Stabilized Ag Nanocluster Fluorophores. *J. Am. Chem. Soc.* **2008**, *130*, 5038–5039.
9. Yeh, H. C.; Sharma, J.; Han, J. J.; Martinez, J. S.; Werner, J. H. A DNA-Silver Nanocluster Probe That Fluoresces upon Hybridization. *Nano Lett.* **2010**, *10*, 3106–3110.
10. Gwinn, E. G.; O'Neill, P.; Guerrero, A. J.; Bouwmeester, D.; Fygenson, D. K. Sequence-Dependent Fluorescence of DNA-Hosted Silver Nanoclusters. *Adv. Mater.* **2008**, *20*, 279–283.
11. Guo, W. W.; Yuan, J. P.; Wang, E. K. Oligonucleotide-Stabilized Ag Nanoclusters as Novel Fluorescence Probes for the Highly Selective and Sensitive Detection of the Hg^{2+} Ion. *Chem. Commun.* **2009**, 3395–3397.
12. Chen, W.-Y.; Lan, G.-Y.; Chang, H.-T. Use of Fluorescent DNA-Templated Gold/Silver Nanoclusters for the Detection of Sulfide Ions. *Anal. Chem.* **2011**, *83*, 9450–9455.
13. Yang, S. W.; Vosch, T. Rapid Detection of MicroRNA by a Silver Nanocluster DNA Probe. *Anal. Chem.* **2011**, *83*, 6935–6939.
14. Sharma, J.; Yeh, H.-C.; Yoo, H.; Werner, J. H.; Martinez, J. S. Silver Nanocluster Aptamers: *in Situ* Generation of Intrinsically Fluorescent Recognition Ligands for Protein Detection. *Chem. Commun.* **2011**, *47*, 2294–2296.

15. Nakatani, K. Chemistry Challenges in SNP Typing. *ChemBioChem* **2004**, *5*, 1623–1633.
16. Lyamichev, V.; Mast, A. L.; Hall, J. G.; Prudent, J. R.; Kaiser, M. W.; Takova, T.; Kwiatkowski, R. W.; Sander, T. J.; de Arruda, M.; Arco, D. A.; *et al*. Polymorphism Identification and Quantitative Detection of Genomic DNA by Invasive Cleavage of Oligonucleotide Probes. *Nat. Biotechnol.* **1999**, *17*, 292–296.
17. Wilhelmsson, L. M.; Norden, B.; Mukherjee, K.; Dulay, M. T.; Zare, R. N. Genetic Screening Using the Colour Change of a PNA-DNA Hybrid-Binding Cyanine Dye. *Nucleic Acids Res.* **2002**, *30*, e3.
18. Wang, D. G.; Fan, J. B.; Siao, C. J.; Berno, A.; Young, P.; Sapolsky, R.; Ghandour, G.; Perkins, N.; Winchester, E.; Spencer, J.; *et al*. Large-Scale Identification, Mapping, and Genotyping of Single-Nucleotide Polymorphisms in the Human Genome. *Science* **1998**, *280*, 1077–1082.
19. Cosnier, S.; Mailley, P. Recent Advances in DNA Sensors. *Analyst* **2008**, *133*, 984–991.
20. Moran, N.; Bassani, D. M.; Desvergne, J. P.; Keiper, S.; Lowden, P. A. S.; Vyle, J. S.; Tucker, J. H. R. Detection of a Single DNA Base-Pair Mismatch Using an Anthracene-Tagged Fluorescent Probe. *Chem. Commun.* **2006**, 5003–5005.
21. Yamana, K.; Fukunaga, Y.; Ohtani, Y.; Sato, S.; Nakamura, M.; Kim, W. J.; Akaike, T.; Maruyama, A. DNA Mismatch Detection Using a Pyrene-Excimer-Forming Probe. *Chem. Commun.* **2005**, 2509–2511.
22. Duprey, J.-L. H. A.; Zhao, Z.-y.; Bassani, D. M.; Manchester, J.; Vyle, J. S.; Tucker, J. H. R. Detection of DNA Base Variation and Cytosine Methylation at a Single Nucleotide Site Using a Highly Sensitive Fluorescent Probe. *Chem. Commun.* **2011**, *47*, 6629–6631.
23. Zeglis, B. M.; Barton, J. K. a Mismatch-Selective Bifunctional Rhodium−Oregon Green Conjugate: a Fluorescent Probe for Mismatched DNA. *J. Am. Chem. Soc.* **2006**, *128*, 5654–5655.
24. Granzhan, A.; Teulade-Fichou, M. P. a Fluorescent Bisanthracene Macrocycle Discriminates between Matched and Mismatch-Containing DNA. *Chem.−Eur. J.* **2009**, *15*, 1314–1318.
25. Guo, W. W.; Yuan, J. P.; Dong, Q. Z.; Wang, E. K. Highly Sequence-Dependent Formation of Fluorescent Silver Nanoclusters in Hybridized DNA Duplexes for Single Nucleotide Mutation Identification. *J. Am. Chem. Soc.* **2010**, *132*, 932–934.
26. Rotaru, A.; Dutta, S.; Jentzsch, E.; Gothelf, K.; Mokhir, A. Selective dsDNA-Templated Formation of Copper Nanoparticles in Solution. *Angew. Chem., Int. Ed.* **2010**, *49*, 5665–5667.
27. Rucker, V. C.; Foister, S.; Melander, C.; Dervan, P. B. Sequence Specific Fluorescence Detection of Double Strand DNA. *J. Am. Chem. Soc.* **2003**, *125*, 1195–1202.
28. Kim, M.-J.; Kim, B.-R.; Kim, H.-T. Investigation of the Cu Binding Site at [dCdG] and [CG] Base Pairs in the Absence of a DNA Backbone. *Chem. Phys. Lett.* **2011**, *505*, 57–64.
29. Andrushchenko, V.; Van De Sande, J. H.; Wieser, H. Vibrational Circular Dichroism and IR Absorption of DNA Complexes with Cu^{2+} Ions. *Biopolymers* **2003**, *72*, 374–390.
30. Vilar-Vidal, N.; Blanco, M. C.; Lopez-Quintela, M. A.; Rivas, J.; Serra, C. Electrochemical Synthesis of Very Stable Photoluminescent Copper Clusters. *J. Phys. Chem. C* **2010**, *114*, 15924–15930.
31. Lisiecki, I.; Billoudet, F.; Pileni, M. P. Control of the Shape and the Size of Copper Metallic Particles. *J. Phys. Chem.* **1996**, *100*, 4160–4166.
32. St-Louis, M.; Tanguay, R. M. Mutations in the Fumarylacetoacetate Hydrolase Gene Causing Hereditary Tyrosinemia Type I: Overview. *Hum. Mutat.* **1997**, *9*, 291–299.
33. Kypr, J.; Kejnovska, I.; Renciuk, D.; Vorlickova, M. Circular Dichroism and Conformational Polymorphism of DNA. *Nucleic Acids Res.* **2009**, *37*, 1713–1725.
34. Yam, V. W.-W.; Cheng, E. C.-C.; Zhou, Z.-Y. A Highly Soluble Luminescent Decanuclear Gold(I) Complex with a Propeller-Shaped Structure. *Angew. Chem., Int. Ed.* **2000**, *39*, 1683–1685.
35. Yam, V. W.-W.; Cheng, E. C.-C.; Cheung, K.-K. A Novel High-Nuclearity Luminescent Gold(I)−Sulfido Complex. *Angew. Chem., Int. Ed.* **1999**, *38*, 197–199.
36. Wu, Z.; Jin, R. On the Ligand's Role in the Fluorescence of Gold Nanoclusters. *Nano Lett.* **2010**, *10*, 2568–2573.
37. Seidel, C. A. M.; Schulz, A.; Sauer, M. H. M. Nucleobase-Specific Quenching of Fluorescent Dyes. 1. Nucleobase One-Electron Redox Potentials and Their Correlation with Static and Dynamic Quenching Efficiencies. *J. Phys. Chem.* **1996**, *100*, 5541–5553.
38. Bahr, M.; Gabelica, V.; Granzhan, A.; Teulade-Fichou, M. P.; Weinhold, E. Selective Recognition of Pyrimidine-Pyrimidine DNA Mismatches by Distance-Constrained Macrocyclic Bis-Intercalators. *Nucleic Acids Res.* **2008**, *36*, 5000–5012.
39. Qin, W. J.; Yung, L. Y. L. Nanoparticle-Based Detection and Quantification of DNA with Single Nucleotide Polymorphism (SNP) Discrimination Selectivity. *Nucleic Acids Res.* **2007**, *35*, e111.
40. Kanjanawarut, R.; Su, X. D. Colorimetric Detection of DNA Using Unmodified Metallic Nanoparticles and Peptide Nucleic Acid Probes. *Anal. Chem.* **2009**, *81*, 6122–6129.
41. Farjami, E.; Clima, L.; Gothelf, K.; Ferapontova, E. E. "Off−On" Electrochemical Hairpin-DNA-Based Genosensor for Cancer Diagnostics. *Anal. Chem.* **2011**, *83*, 1594–1602.